ELSEVIER

Journal of Chromatography B, 695 (1997) 103–111

JOURNAL OF CHROMATOGRAPHY B

Examination of band dispersion during size-selective capillary electrophoresis separations of DNA fragments

Timothy J. Gibson, Michael J. Sepaniak*

Department of Chemistry, University of Tennessee, Knoxville, TN 37996-1600, USA

Abstract

Versatile capillary electrophoresis instrumentation that permits the rapid and precise translation of a laser fluorometric detection zone along the capillary wall has been used to examine the factors which cause band broadening during size-selective separations of DNA fragments. Separations are performed using capillaries containing entangled polymer solutions. The scanning capabilities of this instrumentation facilitates the determination of diffusion coefficients under static conditions without the need to discontinue and reapply an electric field. The ability to rapidly translate the detection zone along the column allows the monitoring of the separation at various points along the capillary which enables the examination of the sources of band dispersion under kinetic conditions. Results from experiments utilizing various concentrations of both high and low molecular mass methyl cellulose polymers as sieving media are presented. It is shown that axial diffusion, even when adjusted for kinetic conditions using the Einstein relationship, does not account for the total observed band variance. Possible explanations for this behavior are presented.

Keywords: Band dispersion; DNA

1. Introduction

A demand for faster, more efficient methods for DNA fragment analysis has resulted in extensive research examining the use of capillary electrophoresis (CE) as an alternative to slab-gel electrophoresis [1–4]. Slab-gels are cumbersome to prepare and load with samples. In addition, poor heat dissipation leads to extensive thermal gradients which rapidly degrades efficiency and often results in poor resolution. To minimize Joule heating, slab-gel electrophoresis is performed at relatively low fields (10 V/cm) which results in long analysis times. Conversely, CE employs narrow-bore capillaries which allow for better heat dissipation, thus, higher applied fields can be used (usually >200 V/cm). This results in a much quicker analysis and improved peak efficiency and resolution. The use of ultrathin slab gels has been studied, either as an alternative to capillary gels [5–7] or as a secondary source of separation [8]. However, several problems still exist before the use of ultrathin gels become preferential to CE and resolution and efficiency are still generally better in CE.

Capillary gel electrophoresis (CGE) has been thoroughly investigated as an alternative to slab-gel electrophoresis [9–12] but lately much attention has been focused on the use of dilute soluble polymer solutions as sieving media in a technique often termed size-selective capillary electrophoresis (SSCE) [13–15]. In CGE, the gel matrix is covalently bound to the capillary wall which makes it very susceptible to changes in temperature and pH [9,16]. However, because soluble polymer solutions

*Corresponding author.

PII S0378-4347(97)00212-0

are not chemically linked to the capillary walls, they are not as susceptible to these perturbations. Also, because these polymer solutions may be easily flushed and replenished within the capillaries, the lifetime of columns is extended. This also permits the use of different sieving media (changes in selected polymer, molecular mass and concentration) without the need to prepare new columns.

In order to fully benefit from the advantages of CE, operating conditions must be carefully optimized. For example, higher applied fields will decrease analysis time but will eventually lead to a thermal gradient within the capillary; the increase in efficiency resulting from shorter analysis time (less time for diffusion) may become offset by the loss in efficiency due to thermal gradients. Therefore, the applied field which results in the most efficient peaks and best resolution must be found by experimentally determining theoretical plate count at various field strengths [17].

Total peak variance in CE (σ^2_{Total}) may result from a variety of sources including diffusion (σ^2_{diff}), injection variance (σ^2_{inj}), a finite detection volume (σ^2_{det}) and thermal gradients ($\sigma^2_{\Delta\text{Th}}$), to name just a few. The total variance is simply the sum of the individual sources of variance as seen in Eq. (1).

$$\sigma^2_{\text{Total}} = \sigma^2_{\text{diff}} + \sigma^2_{\text{inj}} + \sigma^2_{\text{det}} + \sigma^2_{\Delta\text{Th}} + \sigma^2_{\text{other}} \quad (1)$$

Careful selection of conditions may minimize certain sources of variance. For example, short electromigration injection times and detection zones often render σ^2_{inj} and σ^2_{det} negligible. Generally, diffusion and thermal gradients are considered the most problematic sources of variance in CGE. However, thermal gradients may be minimized by using smaller I.D. columns and low fields (<250 V/cm). Under these conditions, it is generally believed that efficiency is determined by the most fundamental dispersional process, axial diffusion. One possible control of diffusional effects is to use solutions of relatively high viscosities. However, a more important parameter of polymer solutions, namely mesh size, makes it difficult to allow an independent choice of solution viscosity [18]. There are other sources of dispersion to consider (σ^2_{other}) such as variance due to conductivity differences between sample zones and running buffer and also solute–wall interactions. Again, these sources of variance can be minimized by the selection of an appropriate buffer and modifying the column wall in order to suppress electroosmotic flow. Another possible contribution to σ^2_{other} is resistance to mass transfer that results from DNA fragment–entangled polymer interactions.

A method for the determination of diffusion coefficients for proteins has been reported [19]. Briefly, this involves injecting a solute band and electrophoresing without pause. A second injection is performed and the solute band is allowed to migrate a short distance into the column. The field is discontinued for several hours before the field is reapplied and the solute band migrates past the detector. The difference in peak width from these two injections is attributed solely to diffusion during the period of time the field was discontinued. However, the "stopped migration" method employed requires more than one injection in order to obtain sufficient data. Reproducibility may become a problem if variance due to electrokinetic injections does not remain constant for subsequent injections. Also, given the conformational dynamics of DNA during electrophoresis in a polymer solution, the diffusion coefficient measured under static conditions would not be expected to be the same diffusion coefficient observed under kinetic conditions. Luckey et al. [20] derived an equation for the determination of kinetic diffusion coefficients of DNA fragments in CGE based on the Einstein relationship. This equation utilizes the static diffusion coefficient (D^0) and the relative mobilities at an applied field and at zero field (Eq. (2));

$$D^E = D^0(\mu^E/\mu^0) \quad (2)$$

where D^E is the kinetic diffusion coefficient for an applied field=E, μ^E is the electrophoretic mobility measured at an applied field and μ^0 is the zero-field mobility which is obtained by regression analysis.

In this work, we determine the static diffusion coefficients of selected fragments from a ϕX-174 Hae III digest under truly static conditions by use of scanning CE instrumentation that permits the rapid and precise translation of a laser fluorometric detection zone along the capillary wall [21,22]. Static diffusion coefficients in various methyl cellulose

concentrations are determined. With this instrumentation, we also examined kinetic band dispersion when performing electrophoretic separations of DNA fragments in entangled polymer solutions. The effects of polymer size and concentration on kinetic band dispersion are also presented. We find that the use of a calculated kinetic diffusion coefficient is not sufficient to account for the total dispersion observed at low fields when performing SSCE. At elevated fields, we observe that dispersion increases as thermal gradients begin to predominate at fields >250 V/cm.

2. Experimental

2.1. Materials

Tris(hydroxymethyl)aminomethane, boric acid and ethylenediaminetetraacetic acid (EDTA) were purchased from Sigma (St. Louis, MO, USA) and used to prepare a 45 m*M* (pH 8.5) Tris boric acid–EDTA (TBE) buffer. ϕX-174 DNA Hae III digest, methyl cellulose (monomer mass, $M_n = 100\,000$ and $M_n = 20\,000$), ethidium bromide (EB), acrylamide, ammonium persulfate, N,N,N′,N′-tetramethylethylenediamine (TEMED) and γ-methacryloxypropyltrimethoxysilane (γ-MTMS) were also purchased from Sigma. Fused-silica capillaries (75 μm I.D.×365 μm O.D.) were purchased from Polymicro Technologies (Phoenix, AZ, USA).

2.2. Column preparation

Capillaries were cut to give a total length of 40 cm; a window extending from 9 to 31 cm was prepared by removing the polyimide coating with warm sulfuric acid. The capillary walls were deactivated with linear polyacrylamide using the following procedure modified from a procedure introduced by Hjerten [23]: the capillary was washed with 1.0 *M* NaOH for 1 h, rinsed with water for 10 min, washed with 1.0 *M* HCl for 1 h and rinsed again with water for 10 min. Next, an acidic solution of γ-MTMS (20 ml water+50 μl 6 *M* acetic acid+80 μl γ-MTMS) was flushed through the column for 18 h followed by a rinse with water for 10 min. A solution of 0.25 g acrylamide in 9 ml TBE buffer along with a solution of 0.15 g ammonium persulfate in 10 ml TBE buffer was degassed by bubbling helium through for 30 min. Polymerization was initiated by adding 1 ml of the ammonium persulfate solution along with 7.5 μl TEMED to the acrylamide solution; this solution was then quickly introduced into the column to allow in-situ polymerization for 18 h. The excess polyacrylamide was removed by flushing the column with 10 m*M* H_3PO_4. When columns were not in use, they were stored in 10 m*M* H_3PO_4. Columns prepared in this manner were generally usable for numerous runs over a 3–4 week period.

2.3. Solution preparation

DNA samples were prepared by diluting an aliquot from the stock with 45 m*M* TBE to give a final concentration of 5 μg/ml. Methyl cellulose stock solutions were prepared by heating 100 ml TBE buffer to 90°C while degassing with helium. Solid methyl cellulose was then added with stirring until dissolved. Once dissolved, the solution was placed in an ice bath and stirring continued until the solution became clear. Prior to use, EB was added to diluted methyl cellulose solutions to give a concentration of 2.5 μ*M* and then vacuum degassed. Solution viscosities were measured with an Ostwald viscometer.

2.4. Apparatus

The spatial-scanning capillary electrophoresis instrumentation has previously been described in detail [21]. Briefly, the capillary column is secured onto a plexiglass stage which is mounted onto an optical sled. The sled is fitted into a dovetail rail table and is equipped with a plastic chain which is connected to a stepping motor (Boston Gear, Quincy, MA, USA). Motion control of the stepping motor and data acquisition were performed by use of a PS/2 Model 50 IBM computer equipped with a uCDAS-16G data acquisition board (Keithley Metrabyte, Taunton, MA, USA). A description and the specifications for the laser excitation source and fiber optic detector used in this work can also be found in Ref. [21].

2.5. Methods

Before use, air was flushed through the column to remove the H_3PO_4 solution used during column storage. Next, a low viscosity methyl cellulose (MC) solution (10 μM MC without EB) was flushed through the column. The column was then filled with MC of the desired concentration for studies (e.g., 50 μM MC with EB) and the column was equilibrated at 10 kV for 15 min prior to injection. All injections were performed electrokinetically (500 V/10 s).

For the determination of D^0, a sample plug was injected and an electric field was applied to allow solute migration past the detector. Once the desired bands passed the detector, voltage was discontinued. The bands were then scanned by the precise translation of the column past the detector at a velocity of 1.0 cm/min. The column was repositioned at its initial detection point and subsequent scans were performed in the same manner at selected time intervals. Variances used to calculate D^0 were determined from measuring peak widths at half height with the aid of LabCalc software (Galactic Industries, Salem, NH, USA).

For the determination of kinetic dispersion coefficients, a sample plug was injected and an electric field was applied to allow solute migration past the detector. Once the bands passed the detector, the voltage was discontinued, the time required for band migration was noted and the bands were scanned under static conditions. Generally, this required about a three minute pause in kinetic conditions. The field was reapplied and solute migration resumed for a determined period of time. Before the time required for analyte elution, the polarity of the applied field was reversed and the bands continued to migrate in the column now towards the injection side. Once the bands migrated past the detector, the voltage was discontinued, the total time of band migration was noted and the bands were scanned. This procedure was repeated several more times until a sufficient set of data was obtained.

3. Results and discussion

Fig. 1A shows scans of a selected peak from the DNA digest at selected time intervals. The peak widths are measured in centimeters by converting the time axis into a distance axis using the scan rate velocity of 1.0 cm/min. For a Gaussian peak, the peak width at half-height is related to variance by Eq. (3) which is derived from the formula for a Gaussian peak:

$$W_{1/2} = 2[2\ln 2]^{1/2}\sigma_{\text{total}} \quad (3)$$

Once variance is determined, the diffusion coefficients are determined by use of the Einstein equation:

$$\sigma^2 = 2Dt \quad (4)$$

where t is the time allowed for diffusion. The diffusion coefficient is obtained from the slope of a plot of variance versus time. Fig. 1B is presented in order to show that the manipulations performed during our kinetic diffusion studies do not appreciably alter the Gaussian peak shape and, thus, Eq. (3) may also be used to calculate peak variance for these studies as well.

The use of scanning instrumentation for the determination of static diffusion coefficient is advantageous in that the only source contributing to band dispersion during static conditions is diffusion. Determining static diffusion coefficients by stopped migration techniques requires several injections if a set of data is desired; this introduces variance due to electrokinetic injection techniques that are necessary for DNA fragment analysis. The static diffusion coefficients for the last four fragments of the ϕX-174 digest (603, 872, 1078 and 1353 bp) are indicated on Table 1; the R.S.D. values for these determinations were $<10\%$.

In free solution, the diffusion coefficient can be approximated to be inversely proportional to solvent viscosity by the Stokes–Einstein equation (Eq. (5)).

$$D = (kT)/f \quad (5)$$

where k is the Boltzmann constant, T is the temperature and f is the friction coefficient which is equal to $6\pi\eta Na$ (η is viscosity, N is Avogadros number and a is the molal volume) [24]. Though the expression shown is strictly valid only for spheres, we examined the relation between DNA fragment diffusion coefficients and entangled polymer solution viscosities. We measured the static diffusion coefficients for

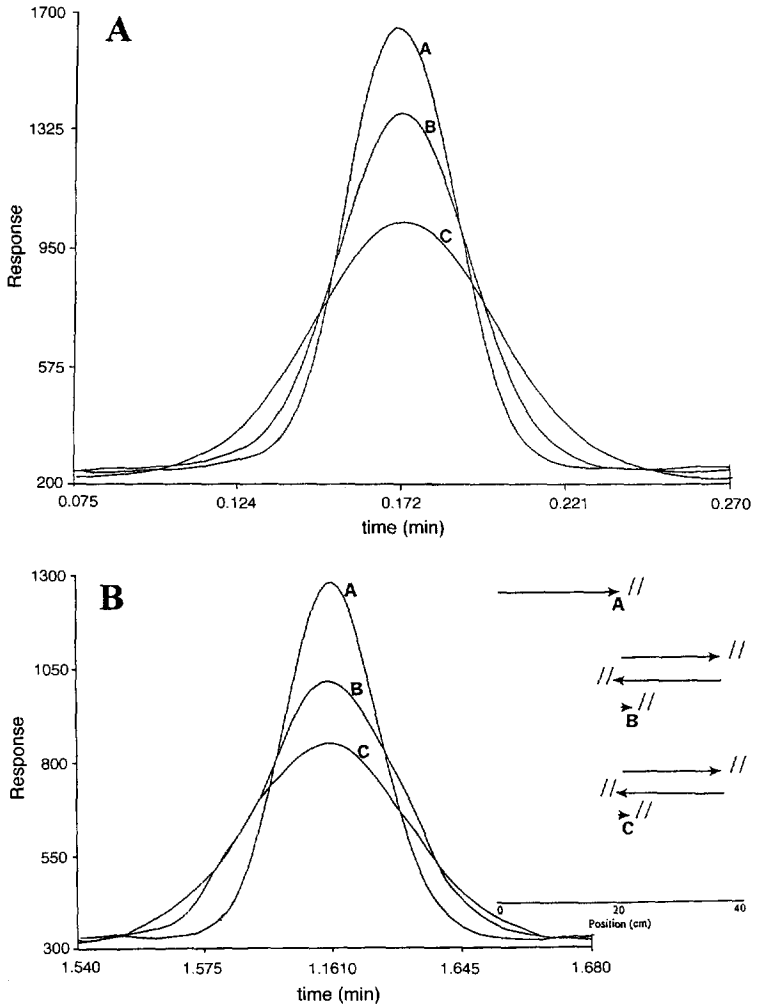

Fig. 1. (A) Scans performed for the determination of static diffusion coefficients. Scans depicted are of a selected peak (1353 bp) from ϕX-174 Hae III digest separated in 840 μ*M* methyl cellulose (M_n = 20 000) in 45 m*M* TBE. Scan rate = 1.0 cm/min; scans were performed at times of (A) 0 min; (B) 27 min and (C) 94 min. (B) Scans performed for the determination of dispersion coefficients. Scans depicted are of a selected peak (603 bp) from ϕX-174 Hae III digest separated in 50 μ*M* nethyl cellulose (M_n = 100 000) in 45 m*M* TBE at a field of 285 V/cm. Scan rate = 1.0 cm/min. The legend indicates the experimental procedure. The first scan was performed after electrophoresis for 6 min (A); the field was reapplied to allow solute migration to 38 cm, the polarity was reversed until the solutes migrated back towards the injection side beyond the detection zone, the polarity was reversed again and the solute band migrated past the detector; the applied field was paused for the second scan at 13 min (B); this was repeated and a third scan after 20 min was obtained (C).

selected fragments in various methyl cellulose solutions and found that the Stokes–Einstein equation is not valid for oligonucleotides in entangled polymer solutions (Fig. 2). In fact, the slope of the line changes sharply at the entanglement threshold for this polymer. From this plot, one can see the difficulty in predicting the diffusion coefficient based on established equations. Therefore, we conclude that the best way to determine static diffusion coefficients when using polymer solutions is to experimentally measure them.

Again, because of the various migration models of DNA fragments in entangled polymers during CE, one would predict that the diffusion coefficients are not the same under kinetic conditions as when under static conditions. Luckey et al. [20] derived a

Table 1
Diffusion/dispersion coefficients (10^{-8} cm^2/s)

	603 bp[a]	603 bp[b]	872 bp	1078 bp	1353 bp
D^0	2.20	3.52	1.62	1.31	0.868
D^{50} (c)	2.30	3.68	1.71	1.38	0.907
D^{50} (o)	4.80	5.85	4.67	5.63	5.40
% acc.	47.9	62.9	36.6	24.5	16.8
D^{105} (c)	2.43	3.83	1.79	1.47	0.978
D^{105} (o)	11.8	6.88	14.2	14.6	13.0
% acc.	20.6	55.7	12.6	10.1	7.5
D^{170} (c)	2.53	4.02	2.00	1.66	1.10
D^{170} (o)	16.4	8.85	18.5	14.4	17.5
% acc.	15.4	45.4	10.8	11.5	6.3
D^{235} (c)	2.78	4.12	2.23	1.84	1.23
D^{235} (o)	18.1	12.3	19.5	19.6	19.1
% acc.	15.3	33.5	11.4	9.4	6.4
D^{285} (c)	2.81	4.33	2.26	1.87	1.25
D^{285} (o)	21.8	14.0	27.4	23.9	24.8
% acc.	12.9	30.9	8.2	7.8	5.0
D^{350} (c)	2.89	4.41	2.33	1.93	1.29
D^{350} (o)	23.4	18.4	28.6	24.4	24.6
% acc.	12.3	24.0	8.1	7.9	5.2
D^{415} (c)	3.07	4.80	2.49	2.06	1.38
D^{415} (o)	36.0	27.1	34.9	34.1	33.2
% acc.	8.5	17.7	7.1	6.0	4.1

[a] Data from experiments in 50 μM MC ($M_n = 100\,000$).
[b] Data from experiments in 840 μM MC ($M_n = 20\,000$).
D^{50} (c) = calculated diffusion coefficient at a field of 50 V/cm.
D^{50} (o) = observed diffusion coefficient at a field of 50 V/cm.
% acc. = % dispersion accounted for by calculated kinetic diffusion.

relationship relating the two diffusion coefficients based on the mobility of the DNA fragments (see Eq. (2)). Using a 50 μM MC solution ($M_n = 100\,000$), the fragment mobilities were measured at various fields and are compiled in Table 2. The linear portion of this relationship is observed at low fields and, thus, the zero-field mobility used in subsequent calculations is extrapolated from the portion of the graph corresponding to low applied fields (<200 V/cm). At each field, the expected kinetic diffusion coefficients were calculated and are indicated in Table 1. We determined the peak variance of these fragments during CE at these fields and concluded that the calculated kinetic diffusion coefficient does not substantially account for the total variance observed; therefore, we determined a "dispersion" coefficient in the same manner in which the diffusion coefficients were determined. Two significant trends in this data are observed. First, as the fragment size becomes larger, the percent dispersion accounted for by the calculated kinetic diffusion coefficient becomes less. Also, as the applied field is increased, the percent dispersion accounted for by diffusion becomes less, even at low fields.

The concentration of low molecular mass methyl cellulose ($M_n = 20\,000$) that will give a comparable pore size as a 50 μM methyl cellulose ($M_n = 100\,000$) solution was determined to be 840 μM

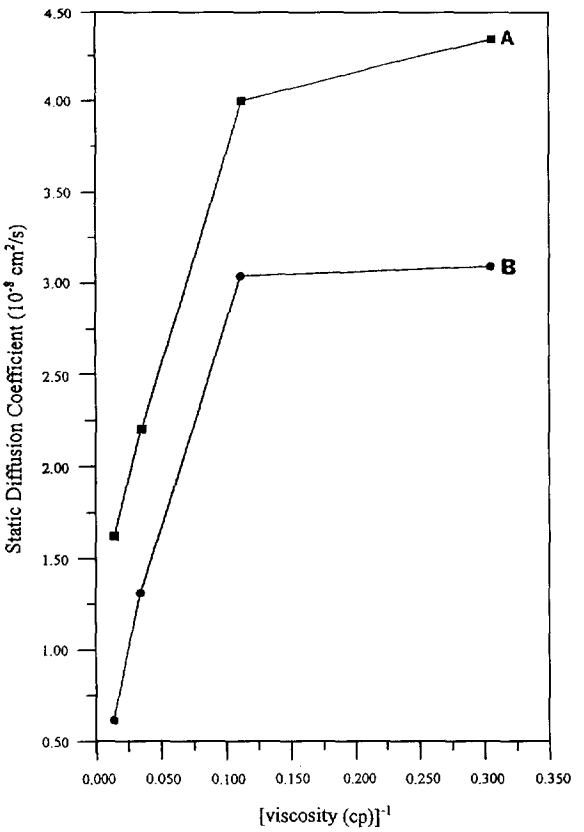

Fig. 2. Inverse proportionality of static diffusion and viscosity is not observed in entangled polymer solutions. The static diffusion coefficient for the 603 bp fragment (A) and the 1078 bp fragment (B) were measured in the following methyl cellulose (M_n = 100 00) solutions (respective viscosities indicated in parentheses): 20 μ*M* (3.29 cp), 35 μ*M* (9.13 cp), 50 μ*M* (29.2 cp) and 70 μ*M* (73.1 cp).

based on polymer mesh size equations [25]. The same experiment was repeated, again comparing expected kinetic diffusion coefficients with observed dispersion coefficients, using the low molecular mass polymer. The same general trends were observed; that is, the percent dispersion accounted for by the calculated kinetic diffusion coefficient became less as the fragment size became larger and as the applied field was increased. However, when comparing the data from the two polymer studies, the high molecular mass polymer showed significantly more non-diffusional dispersion than what was observed in the low molecular mass polymer; this is shown in Table 1 for the 603 base pair fragment.

Table 2
Mobility of DNA fragments in methyl cellulose solutions (data reported at 10^{-4} cm^2/V s)

Field (V/cm)	603 bp	872 bp	1078 bp	1353 bp
50 μ*M* Methyl cellulose (M_n = 100 000)				
415	2.25	2.20	2.16	2.13
350	2.11	2.06	2.02	1.99
285	2.05	2.00	1.96	1.93
235	2.03	1.97	1.93	1.90
170	1.85	1.77	1.74	1.70
105	1.77	1.58	1.54	1.51
50	1.68	1.51	1.44	1.40
μ^0	1.61	1.45	1.35	1.30
840 μ*M* Methyl cellulose (M_n = 20 000)				
415	1.84	1.81	1.78	1.75
350	1.69	1.65	1.62	1.61
285	1.66	1.62	1.59	1.58
235	1.58	1.52	1.50	1.49
170	1.54	1.48	1.45	1.44
105	1.47	1.39	1.36	1.34
50	1.41	1.31	1.26	1.23
μ^0	1.35	1.25	1.21	1.19

The rapid band dispersion observed during CE is most complex and cannot be attributed solely to longitudinal diffusion. Furthermore, the equation proposed by Luckey et al. [20] for kinetic diffusion coefficient determinations in CGE does not appear to account for a significant portion of band dispersion observed when utilizing entangled polymer solutions (i.e., in SSCE). This is graphically shown in Figs. 3 and 4. Slater et al. [26] further examined sources of band dispersion in CGE and addressed the validity of the kinetic diffusion expression shown in Eq. (2). Their contention is that the Einstein relationship used in the derivation by Luckey et al. is not appropriate for the non-equilibrium events occurring in these CGE separations of DNA fragments. They derive an expression that predicts that the longitudinal diffusion coefficient (D_x) initially increases as the applied field increases; however, as the field becomes stronger, the effect on molecular orientation of the DNA fragments is such that they become more rigidly elongated. This orientation effect begins to cause a decrease in D_x as the orientation becomes saturated. These researchers also present calculations that indicate there is a maximum in D_x when plotted versus base pair number. Slater et al. utilized scaled

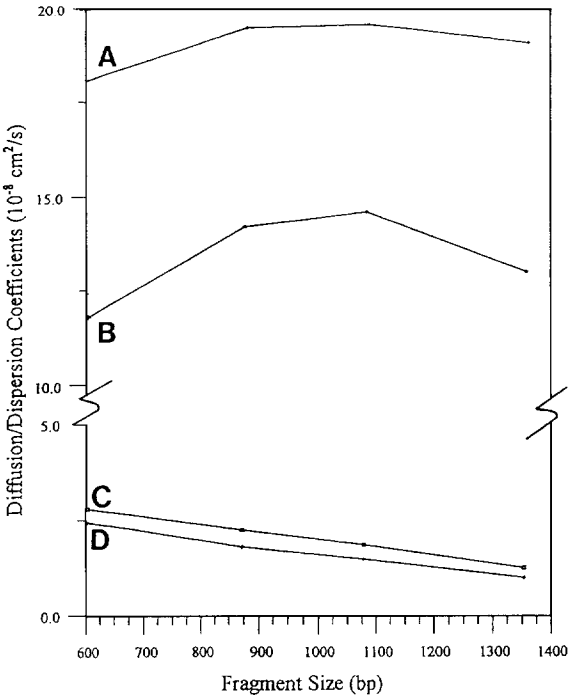

Fig. 3. Effect of fragment size on diffusion and dispersion is shown at two selected field strengths. Dispersion coefficients are shown at (A) 235 V/cm and (B) 105 V/cm; the kinetic diffusion coefficients calculated for (C) 235 V/cm and (D) 105 V/cm are also represented.

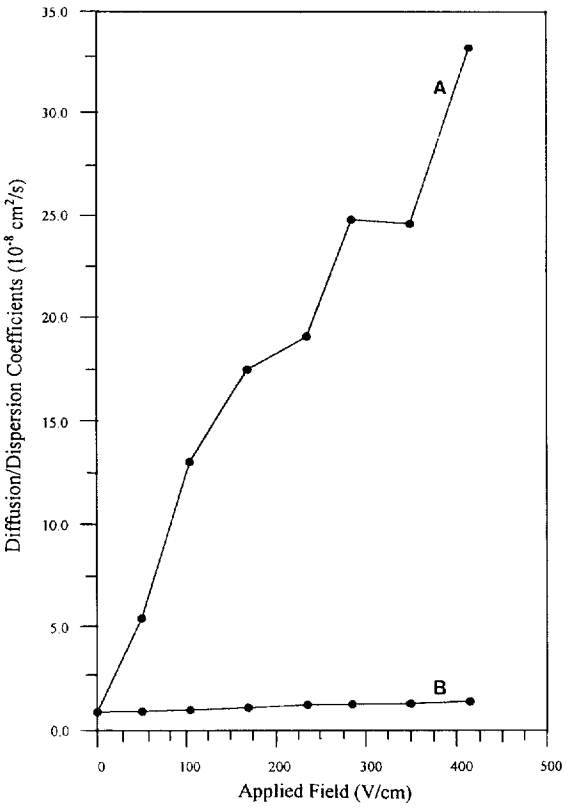

Fig. 4. Observed dispersion coefficient (A) and the calculated kinetic diffusion coefficient (B) versus applied field is shown for the 1353 base pair fragment.

field and base pair parameters and CGE conditions that cannot be easily extrapolated to our SSCE conditions. Nevertheless, our plots of dispersion coefficient versus base pair number for the larger fragments in the test sample appear to exhibit a weak maximum (see Fig. 3A,B). The plot of dispersion coefficient versus field for the 1353 base pair fragment shown in Fig. 4A does not exhibit a clear maximum. Although, it appears that the slope of that plot decreases for mid-range fields, then increases dramatically for the highest field, presumably due to the onset of severe thermal dispersion.

Luckey et al. [20] contend that as a fragment elongates in an applied field, the transverse diffusion coefficient (D_y, perpendicular to the capillary axis and the applied field) decreases. This should exacerbate problems with the thermal gradients that occur at high fields since rapid transverse diffusion reduces the dispersive effects of thermal gradients. Again, Slater et al. [26] come to a different conclusion concerning the magnitude of and trends in D_y. Their derivation indicates that D_y can be relatively large and hence thermal gradients are less problematic than predicted by Luckey et al. Our experimental results do not shed much light on this controversy. However, the dispersion coefficient observed at very high fields shown in Table 1 and Fig. 4 clearly indicate the onset of thermal dispersion.

The DNA fragment–entangled polymer interactions which lead to separation in SSCE were discussed by Barron et al. [27]. They state that the retardation of mobility caused by these interactions is what actually permits the separation of fragments; thus, the larger the fragments, the more sites for it to become entangled and, consequently, the lesser the observed mobility. They further state that the larger the entangled polymer chain, the more of a frictional

drag it exerts on the fragment and, again, the more retarded the mobility will be. It may be concluded that these non-equilibrium interactions involving entanglement–disentanglement are indeed a significant contribution to band dispersion during CE. These fragment–polymer interactions may be considered to be similar to resistance to mass transfer in other chromatography methods. Fragments become entangled and "drag" polymers in various discrete steps during CE. This conclusion is consistent with the trends observed in our data in Table 1 and with the observations stated by Barron et al.; the larger fragments and solutions of the higher molecular mass entangled polymer showed the greatest dispersion.

We conclude that certain assumptions made for CGE may not be valid for polymer solutions. The sources of dispersion that are significant in CGE are also significant in polymer solutions but the dynamics of the separation process in the two systems differ and this causes the extent of dispersion by these sources to not be equal. The trends in our data show some agreement with derivations offered by Slater et al. However, the trends we observe might also be qualitatively described by a traditional chromatographic resistance to mass transfer argument. Clearly, the issue of band dispersion in DNA separations is scientifically intriguing. However, we must end with a humorous note put forth by Righetti on this topic, "As luck goes, most authors have ignored these issues so far and lived happily with their CZE results" [28].

Acknowledgments

This work was sponsored by the Division of Chemical Sciences, Office of Basic Sciences, United States Department of Energy, under grant DE-FG02-96ER14609 with the University of Tennessee, Knoxville. Support was also contributed by Merck and Company and Pfizer Research Central. The authors would also like to thank Drs. T.D. Staller and B.K. Clark for their assistance with the programming used in data acquisition.

References

[1] A.S. Cohen, D. Najarian, J.A. Smith, B.L. Karger, J. Chromatogr. 458 (1988) 323.
[2] D.N. Heiger, A.S. Cohen, B.L. Karger, J. Chromatogr. 516 (1990) 33.
[3] A. Guttman, N. Cooke, Anal. Chem. 63 (1991) 2038.
[4] K.J. Ulfelder, H.E. Schwartz, J.M. Hall, F.J. Sunzeri, J. Anal. Biochem. 200 (1992) 260.
[5] R.L. Brumley, L.M. Smith, Nucl. Acids Res. 19 (1991) 4121.
[6] A.J. Kostichka, M.L. Marchbanks, R.L. Brumley, H. Drossman, L.M. Smith, Bio/Technology 10 (1992) 78.
[7] D. Chen, M.D. Peterson, R.L. Brumley, M.C. Giddings, E.C. Buxton, M. Westphall, L. Smith, L.M. Smith, Anal. Chem. 67 (1995) 3405.
[8] Y. Liu, J.V. Sweedler, Anal. Chem. 68 (1996) 3928.
[9] A. Guttman, N. Cooke, J. Chromatogr. 559 (1991) 285.
[10] H. Swerdlow, J.Z. Zhang, D.Y. Chen, H.R. Harke, R. Grey, S. Wu, N.J. Dovichi, C. Fuller, Anal. Chem. 63 (1991) 2835.
[11] H.R. Harke, S. Bay, J.Z. Zhang, M.J. Rocheleau, N.J. Dovichi, J. Chromatogr. 608 (1992) 143.
[12] M.J. Navin, T.L. Rapp, M.D. Morris, Anal. Chem. 66 (1994) 1179.
[13] M. Zhu, D.L. Hanson, S. Burd, F. Gannon, J. Chromatogr. 480 (1989) 311.
[14] W.A. MacCreahan, H.T. Rasmussen, D.M. Northrup, J. Liq. Chromatogr. 15 (1992) 1063.
[15] B.K. Clark, M.J. Sepaniak, J. Microcolumn Sep. 5 (1993) 275.
[16] A. Guttman, J. Horvath, N. Cooke, Anal. Chem. 65 (1993) 199.
[17] D.A. McGregor, E.S. Yeung, J. Chromatogr. A 652 (1993) 67.
[18] B.K. Clark, C.L. Nickles, K.C. Morton, J. Kovac, M.J. Sepaniak, J. Microcolumn Sep. 6 (1994) 503–513.
[19] Y. Walbroehl, J.W. Jorgenson, J. Microcolumn Sep. 1 (1989) 41.
[20] J.A. Luckey, T.B. Norris, L.M. Smith, J. Phys. Chem. 97 (1993) 3067.
[21] B.K. Clark, T. Vo-Dinh, M.J. Sepaniak, Anal. Chem. 67 (1995) 680.
[22] B.K. Clark, M.J. Sepaniak, J. Microcolumn Sep. 7 (1995) 593.
[23] S. Hjerten, J. Chromatogr. 347 (1985) 191.
[24] P.W. Atkins, Physical Chemistry, W.H. Freeman, New York, 4th ed., 1990.
[25] J.L. Viovy, T. Duke, Electrophoresis 14 (1993) 322.
[26] G.W. Slater, P. Mayer, P.D. Grossman, Electrophoresis 16 (1995) 75.
[27] A.E. Barron, H.W. Blanch, D.S. Soane, Electrophoresis 15 (1994) 597.
[28] P.G. Righetti (Editor), Capillary Electrophoresis in Analytical Biotechnology, CRC Press, Boca Raton, FL, 1996.